Acta Technica *63* No. 1B/2018, 1–8

Statistical investigation of solar effect in the descending period based by empirical data from precursors of Demeter satellite[1]

M. A. Abasi[2], M. Masnadi Shirazi[1]

Abstract. In the last decade it has been shown that disruptions on the ionospheric parameters have the most important impact in the studies related to the prediction of earthquakes. Therefore, researches in the field of ionospheric perturbations have particular importance in recent years. In this paper, the density of positive ions of oxygen, hydrogen, helium and ion temperature have been selected among the ionospheric parameters. Since solar activities and geomagnetic noises were at high level during early months of 2005 (especially in January) and late month of 2006, so sampling of the four components is performed during those periods. In this paper the main source of sampling is IAP sensor of Demeter satellite which is considered as measurement source. The error between Demeter measurement source and IRI model will be considered as disturbance occurred by solar activities. It is shown that Nakagami statistical model fits very well on the disturbances functions, and by using ML (Maximum Likelihood) method, Nakagami distribution parameters have been estimated. Finally we confirm the accuracy of Nakagami statistical model by using Pearson-Chi-Square goodness of fitness test.

Key words. IAP, Demeter, IRI, maximum likelihood, Nakagami statistical model, solar activity, Pearson-Chi square.

1. Introduction

In several works, many factors such as internal gravity waves (IGW), earthquakes, coupling of ionospheric layer with low-altitude layers and solar activities have been recognized as disturbance factors for the ionospheric parameters, see [1–3]. In addition to ion composition other parameters of ionospheric layer like critical frequency

[1]Authors acknowledge to the online IRI website (http://iri.gsfc.nasa.gov) and Demeter website (http://demeter.cnr8-orleans). Thanks to Dr. Britzia and special thanks to Dr. Masnadi Shirazi and Dr. Sharzeyi that presented very useful guide in this project.

[2]Communications and Electronic Engineering Department. International Division of Shiraz University

(fof2), electron density (ne), TEC (total electron content) and ion temperature can be changed due to disturbance factors [4–6]. In recent years, numerous researches have been conducted on the critical frequency changes and electron density (ne) perturbations as the key of the ionospheric anomalies.

1.1. Determine sampling time due to maximum solar effects between cycle 23 and 24

The main focus of this paper for selecting the sampling times (during 2004–2011) is on the period that solar activities and geomagnetic noises were in their peaks. The other unknown noises except solar activities have small role among the high influence of solar activities. Another point is 27 days periodic time of sun that we considered for sampling. Initially, for determining this periodic time observe the situation of R and $F_{10.7}$ in the following figures (Figs. 1 and 2). Then sampling has been done when our common chosen indices were at the maximum of themselves.

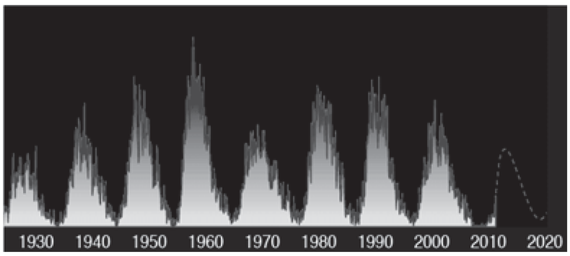

Fig. 1. Variations of sunspots (R) during the years 1930 to 2011

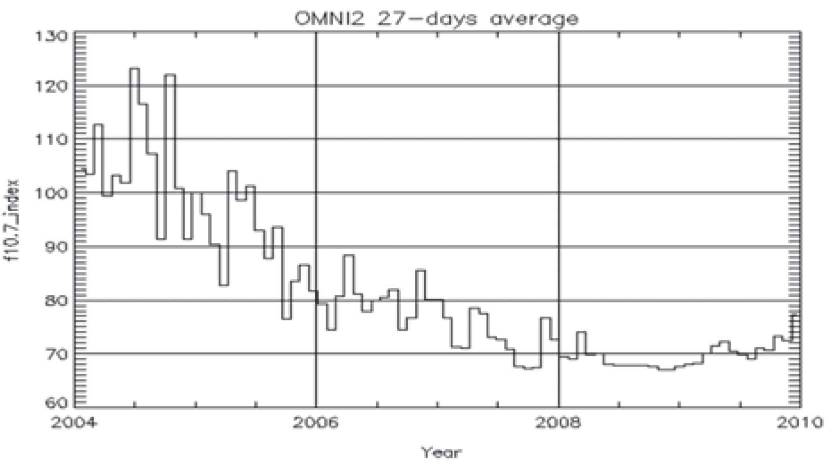

Fig. 2. Variations of 27 days-average of $F_{10.7}$ during the years 2004 to 2010

Figure 3 shows the relationship between R and geomagnetic activity mentioned in [6], based on NOAA database.

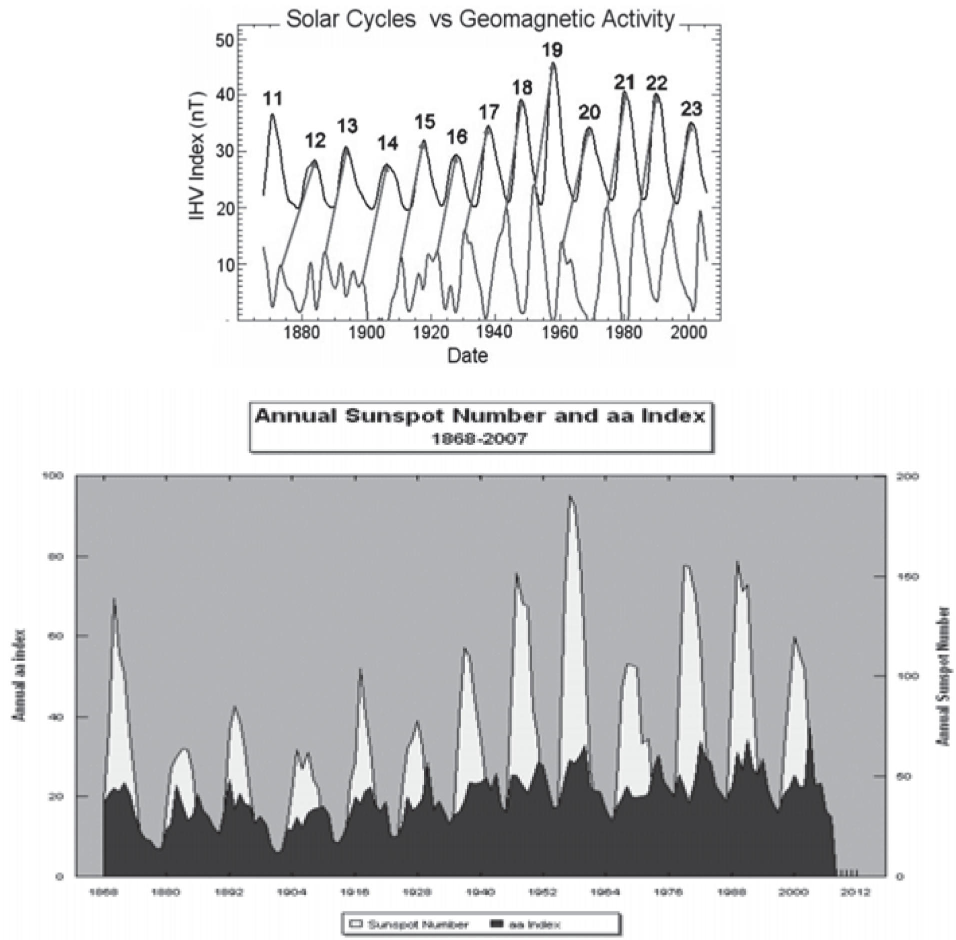

Fig. 3. Variations of the relationship R with geomagnetic activities and A_p during solar cycles

Due to deep look at the years 2004 to 2011 and applying the mentioned restrictions, years 2005 and 2006 in the first step have been selected. In the second step the k_{p} changes has been collected from the NOAA database for determining the 27 day periodic time of sampling during months of two mentioned years (2005-2006). Diagram of k_{p} variation's is shown in Fig. 4.

Eventually, 1^{st}, 5^{th} and 9^{th} months of 2005 and last month of 2006 were selected by authors trough the extensive studies about the solar indices and considered complex relationship between the solar activities and other disruption factors such as intensity of the geomagnetic field. According to the 27-day period of sun, data has been recorded in 27 day intervals from IAP sensor of Demeter satellite.

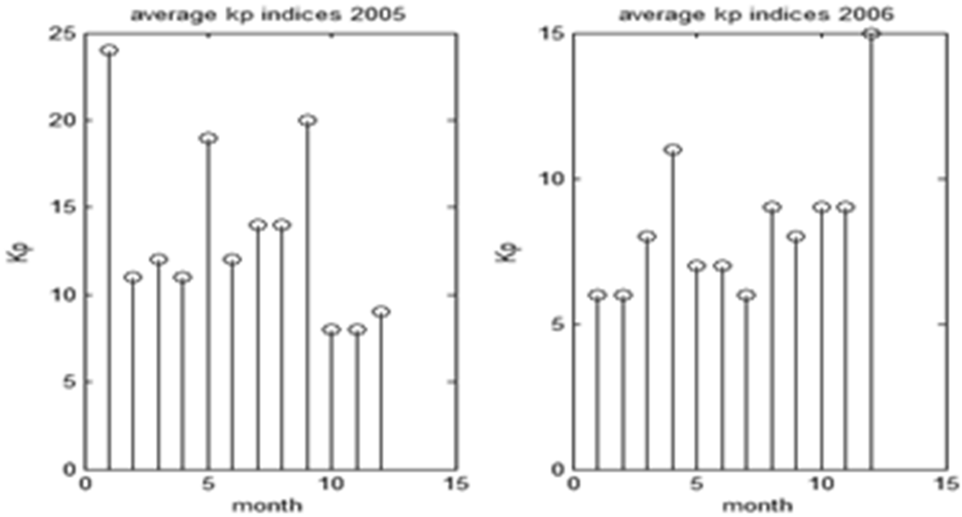

Fig. 4. Time diagram of average changes $\sum k_{\mathrm{p}}$ during 2005–2006

2. Data

According to the mentioned total description in section 1 finally for approximately 2500 initial data were obtained through the IAP sensor of Demeter satellite during 2005–2006. In this paper, our focus is on modeling the ionospheric anomalies that occurs by maximum solar effects between solar cycle 23 and 24 on the local area (Iran). In the first process a local filter designed on the preliminary data after removing the periods of earthquake in Iran during 2005–2006. Iran longitude is between 44–65° east degree and Iran latitude is between 25–40° north degrees. According to the peak of solar activity in January 2005 and lack of Demeter data in the geographic range of Iran during the mentioned period of January, an amount of ε (close to 3°) was added to intended geographical degree.

The geographic limitations are given in Table 1.

Table 1. Local geographic limitation

Latitude	Longitude	Local filter range
minimum	$25-\varepsilon$	$44-\varepsilon$
maximum	$40+\varepsilon$	$60+\varepsilon$

3. Simulation of statistical function fitness and ML estimation

In this paper, ML (Maximum Likelihood) parametric estimation method has been used for fitting proper statistical model on random vectors. Also we utilized random vectors histogram information for better analysis in Fig. 5. Using the histogram is one of the most common and simple methods for recognition initial necessary information. According to the random data scattering of each vector, number of histogram's bin can be increased to a closer examination. The amount of y axis in the histogram indicates number of random variables of $\overline{e}_i$ in each of bins. Finally, with regard to the histogram of random vectors $\overline{e}_i$, before applying any algorithms, two following points are remarkable:

1. All vector components ($\overline{e}_i$) are independent from each other and samples start from zero to N-Symbol (157). In this case a more accurate comparison between vectors $\overline{e}_i$ ultimately achieves a more comprehensive statistical analysis.

2. Each vector has descending approximately trend similar to the periodic changes of solar component, and it shows the influence of solar activities on the selected parameters.

If the error vector $\overline{e}_4$ is a random vector from Gaussian family, which in the next sections will be evaluated more, in this part of study μ (mean of Gaussian distribution) and σ^2 (variance of Gaussian distribution) will be estimated by using the ML estimation method and compare with histogram $\overline{e}_4$.

The likelihood function is

$$L = f\left(\overline{e}_4, \mu_1, \sigma_1\right) \sim N\left(\hat{\mu}_1, \hat{\sigma}_1\right) = \prod_{i=1}^{N} \frac{1}{\sqrt{2\pi\hat{\sigma}_1^2}} \exp\left[-\frac{(e_{i4} - \hat{\mu}1)}{2\hat{\sigma}_1^2}\right] . \tag{1}$$

ML estimation: $\{\hat{\mu}_1, \hat{\sigma}_1\} \leq \{\operatorname{argmax}(L)\}_{\mu,\sigma\in\Omega}$

$$\begin{cases} \text{a) } \frac{\partial L}{\partial \mu} = 0 \to \ \hat{\mu}_1 = \ \hat{\mu}_{\text{ml}} \\ \text{b) } \frac{\partial L}{\partial \sigma} = 0 \ \to \hat{\sigma}_1 = \ \hat{\sigma}_{\text{ml}} \end{cases} \quad \frac{\partial Lnf}{\partial \mu} = 0 \ \to \ \sum_{i=1}^{N} -\frac{(e_{4i} - \hat{\mu}_1)^2}{\hat{\sigma}_1^2} = 0$$

$$\begin{cases} \hat{\mu}_{1\text{ml}} = \frac{1}{N}\sum_{i=1}^{N} e_{4i} \\ \hat{\sigma}_{1\text{ml}} = \frac{1}{N}\sum_{i=1}^{N} (e_{4i} - \hat{\mu}_{1\text{ml}})^2 \end{cases} \quad \frac{\partial Lnf}{\partial \sigma} = 0 \ \ \to \sum_{i=1}^{N}\left[-\frac{1}{2\hat{\sigma}_1^2} + \frac{(e_{4i} - \hat{\mu}_1)^2}{2(\hat{\sigma}_1^2)^2}\ \right] = 0$$

In ML method unknown parameters are estimated such that the distribution function is in its most optimal case properties. According to equation (1) and monotonic of exponential function, finally $\hat{\mu}_{\text{ml}}$ and $\hat{\sigma}_{\text{ml}}$ were obtained for random vector $\overline{e}_4$. After that we can fit normal distribution to the $\overline{e}_4$ as the following figure (Fig. 5).

$$\hat{\mu}_{\text{ml}} = 190.4, \ \ \hat{\sigma}_{\text{ml}} = 147.6\,. \tag{2}$$

3.1. Simulation of fitness models

In statistics and probabilities science, shape parameter variations can change the general framework of density function. Shape parameter in this paper has a great

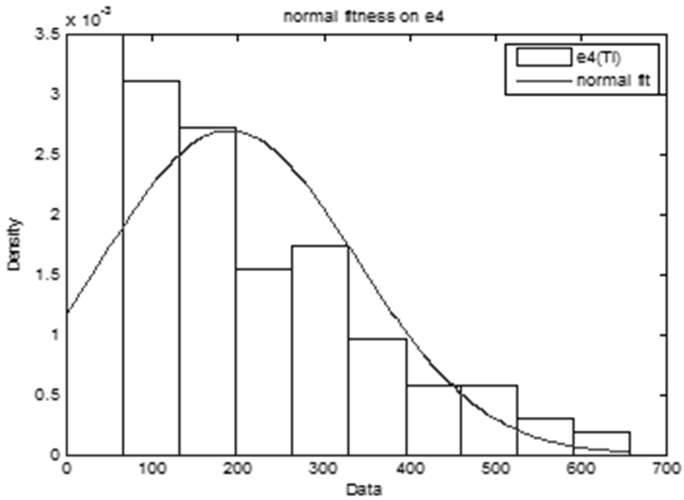

Fig. 5. Normal distribution fitness on $\overline{e}_4$ (disturbances of ion temperature

impact to fitting statistical model on the error vectors. Hence standard error of estimation for the shape parameter is one of the criteria that will be evaluated in simulations. Since anomalies of ion temperature is completely independent from positive ions, $\overline{e}_4$ in the beginning have been selected for simulations similar to the previous section as shown in Fig. 6. Also for better analysis, ML estimation's std-error of shape parameters is gathered in Table 3. The amount of std-error of estimation can be obtained by using different formulas; the below one is one of the more common formulas.

$$\text{Std} - \text{error of estimation} = \sqrt{\frac{\sum_{i=1}^{N} (x_i - \hat{x}_i)^2}{N-2}}\,. \tag{3}$$

Table 3. Estimated values by the ML method, kind of that parameter and amount of std-error of estimation

Statistic fitness model on $\overline{e}_4$	MLE parameters	Kind of estimate parameters	Std-error
Nakagami	$\hat{mu} = 0.48$	Shape parameter	0.04
Generalized-extreme value	$\hat{mu} = 0.197$	Shape parameter	0.09
Weibull	$\hat{mu} = 1.23$	Shape parameter	0.07
Birnbaum-Saunders	$\hat{mu} = 1.436$	Shape parameter	0.086
Gamma	$\hat{mu} = 1.336$	Shape parameter	0.13

According to graphical simulation of multi-statistical models and more comprehensive analysis of the Table 3, we have simulated all proper models. Eventually we claimed Nakagami distribution that in terms of both graphically in simulator environment and the amount of Std-err (.04) has been more appropriate than other desire statistical models for the ionospheric anomalies in terms of ion temperature

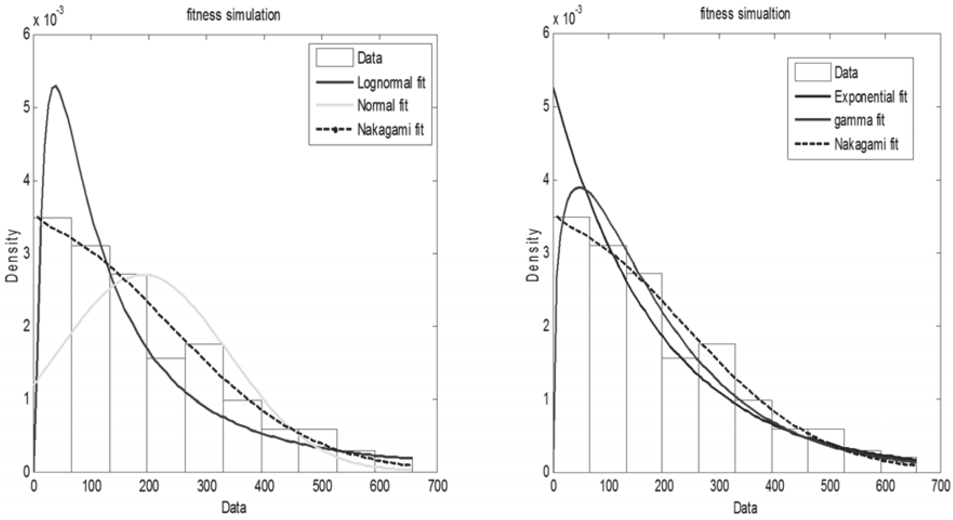

Fig. 6. Fitness simulations of proper distributions on $\overline{e}_4$

variations. In further section we confirmed it for all 4 components that have been selected in this study.

4. Conclusion

Storms and solar geomagnetic activities is one of the most influential factors in creating anomalies on the ionospheric parameters, thus modeling of the effects to predict a natural phenomenon such as earthquake, is particularly important. Given that random changes will appear in plasma parameters, thus obtain an appropriate statistical model which is shows the effect of solar activities at all times is very necessary and useful. With the efforts of the authors of this paper and long-term studies on the parameters selection and statistical sampling time selection, eventually Nakagami statistical model was chosen by applying simulations for the complex effects of solar activities as main factor of anomaly at altitude 600–700 km from Earth's surface. After simulations we evaluated Nakagami model with statistical test and in final step correctness of model for anomalies has been confirmed by reliable results. On the other hand, flexibility of Nakagami statistical model and attention to the similarity of the ionospheric anomalies to a complex telecommunication channel also can be a helpful point for feature works in this field. Generally in results of this paper, authors have been modeled anomaly on the ionospheric layer by Nakagami distribution in statistically terms on the local area (Iran) and between solar cycle 23 and 24 in 2005–2006 when solar effects were at maximum.

References

[1] E. V. Liprovskaya, M. Parrot, V. V. Bagdanov, C. V. Meister, M. V. Rodkin, V. A. Liprovsky: *On variations of foF$_2$ and F-spread before strong earthquakes in Japan.* Natural hazards and earth system sciences *6* (2006), No. 5, 735–739.

[2] C. Akpaça, O. Ünver, Z. Can, K. Bozkurt, K. Kutlu: *Ionospheric TEC model derived from GPS data.* URSI General Assembly and Scientific Symposium, 13–20 August 2011, Istanbul, Turkey, IEEE Conferences (2011), 1–1.

[3] S. McKenna: *Solar radio interference as a function of frequency and time associated ionosphere disturbances.* IEEE Transactions on Communications Systems *11* (1963), No. 1, 79–88.

[4] E. Aa, D. H. Zhang, Z. Xiao, Y. Q. Hao, A. J. Ridley, M. Moldwin: *Modeling ionospheric foF$_2$ by using empirical orthogonal function analysis.* Annales Geophysicae (2011), No. 29, 1501–1515, doi:10.5194/angeo-29-1501-2011.

[5] R. Atulkar, S. Bhardwaj, P. Khatarkar, P. Bhawre, P. K. Purohit1: *Geomagnetic disturbances and its impact on ionospheric critical frequency (foF$_2$) at high, mid and low latitude region.* American Journal of Astronomy and Astrophysics *2* (2014), No. 6, 61–65.

[6] A. Loy, L. Follett, H. Hofmann: *Variations of Q-Q Plots – The Power of our Eyes!.* Journal American Statistician, Statistical Computing and Graphics *70* (2016), No. 2, 202–214, arXiv:1503.02098 [stat.ME].

Received January 23, 2018